ELSEVIER

Nuclear Instruments and Methods in Physics Research A 466 (2001) 464–474

NUCLEAR INSTRUMENTS & METHODS IN PHYSICS RESEARCH Section A

www.elsevier.com/locate/nima

Response of silicon-based linear energy transfer spectrometers: implication for radiation risk assessment in space flights

G.D. Badhwar*, P.M. O'Neill

NASA Lyndon B. Johnson Space Center, Attn: SN, 2101 NASA Road 1, Houston, TX 77058-3696, USA

Received 19 October 2000; accepted 2 November 2000

Abstract

There is considerable interest in developing silicon-based telescopes because of their compactness and low power requirements. Three such telescopes have been flown on board the Space Shuttle to measure the linear energy transfer spectra of trapped, galactic cosmic ray, and solar energetic particles. Dosimeters based on single silicon detectors have also been flown on the Mir orbital station. A comparison of the absorbed dose and radiation quality factors calculated from these telescopes with that estimated from measurements made with a tissue equivalent proportional counter show differences which need to be fully understood if these telescopes are to be used for astronaut radiation risk assessments. Instrument performance is complicated by a variety of factors. A Monte Carlo-based technique was developed to model the behavior of both single element detectors in a proton beam, and the performance of a two-element, wide-angle telescope, in the trapped belt proton field inside the Space Shuttle. The technique is based on: (1) radiation transport intranuclear-evaporation model that takes into account the charge and angular distribution of target fragments, (2) Landau–Vavilov distribution of energy deposition allowing for electron escape, (3) true detector geometry of the telescope, (4) coincidence and discriminator settings, (5) spacecraft shielding geometry, and (6) the external space radiation environment, including albedo protons. The value of such detailed modeling and its implications in astronaut risk assessment is addressed.

Keywords: Silicon dosimeter; Monte Carlo; LET Spectrometer

1. Introduction

The linear response of silicon with energy deposited has led to the development of both single element dosimeters and simple telescopes for measuring the energy deposition spectrum which is then converted into a linear energy transfer (LET), L, spectrum. These telescopes are small and require relatively low power. Single element detectors, such as Liulin [1] and Dose-A [2], have been flown on the Mir orbital station. A two-element telescope, DOSTEL, has been flown on Space Shuttle and the Mir orbital station [3]. Similarly, multi-element telescopes, Real-Time Radiation Measuring Detector (RRMD) [4] and Charged Particle Directional Spectrometer (CPDS) [5] have been flown on a number of Shuttle flights. These telescopes measure the *energy deposition* spectrum in silicon that is

*Corresponding author. Tel.: +1-713-483-5065; fax: +1-281-483-5276.

E-mail address: gautam.d.badhwar1@jsc.nasa.gov (G.D. Badhwar).

0168-9002/01/$ - see front matter
PII: S0168-9002(01)00285-6

converted into a LET spectrum in tissue using a scale factor (=1.31), the ratio of energy loss in keV μm^{-1} in tissue to energy loss in silicon in keV μm^{-1} for a 100 MeV protons. A tissue equivalent proportional counter (TEPC) has been flown on over 25 Shuttle flights [6] and on the Mir station [7]. The TEPC measures the lineal energy (keV μm^{-1}), y, spectrum, and with the substitution of y with L in the definition of quality factor, $Q(L)$, is used to calculate the biologically relevant dose equivalent [8,9]. The y and L spectra are, of course, different, as are the target fragmentation products in silicon and tissue. In addition, the responses of these detectors to neutrons are very different. In order to interpret the silicon measured energy deposition spectrum for estimating dose equivalent, the telescope response must be modeled in detail. In this paper the response of the DOSTEL instrument has been compared to a Monte Carlo-based calculation. This technique can be applied to multi-element silicon telescope equally well.

Singleterry et al. [10] using the Langley Research Center (LaRC) developed semi-analytical radiation transport codes [11,12] to model the response function of the DOSTEL instrument. In this transport code, HZETRN, particles are treated in a straight-ahead approximation. They showed that the main features of the observed LET spectrum could be reasonably well reproduced. These calculations, however, did not take into account the true detector geometry or the energy loss fluctuations leading to a significant discrepancy between the observations and calculations at low LET values. Their calculations also fall off faster at very high LET values than the observations and albedo protons were not considered.

This paper describes a Monte Carlo technique to fully model the behavior of both single element silicon detectors in a proton beam, and the performance of multi-element, wide acceptance LET telescopes, in the geomagnetically trapped proton belt field (South Atlantic Anomaly region). The calculation takes into account: (1) radiation transport, using a intranuclear-evaporation model that includes the target fragment charge, energy, and angular distribution, (2) the Landau–Vavilov distribution of energy deposition allowing for electron escape from detectors, (3) the true geometry of the telescope, treating the detectors as disks and not planes, (4) coincidence and discriminator settings of detector elements, (5) spacecraft shielding geometry, and (6) the external free space radiation environment, including albedo measurements. The contribution of secondary charged pions produced by nuclear interactions of trapped and galactic cosmic radiation with spacecraft shielding is not included; however, it is expected to be very small.

2. Experimental setup

2.1. Instrument description

The DOSTEL is a detector telescope with a full opening angle of 120°. It consists of two 315 μm thick, 27 mm diameter silicon detectors, and 15 mm apart. For an isotropically incident particle flux, the area–solid angle product, $A\Omega$, of the telescope is 8.24 cm^2 sr with the most probable angle of incidence equal to 34° [3]. An energy deposition of >64 keV in both detectors is needed to form a coincidence. It requires minimum proton energy of 6.2 MeV (LET in tissue of 6 keV μm^{-1}) incident perpendicular to the detector surfaces to form a coincidence. The minimum energy increases to 9.1 MeV for an incidence angle of 60°. Thus vertically incident protons with LET> 6 keV μm^{-1} in tissue are rejected. This is also true of many target fragments. The signal from each detector is amplified by two AMPTEK 250 amplifiers, and fed into two 256 analog-to-digital converters covering energy ranges up to 4 and 80 MeV, respectively. The telescope measures the *energy deposited*, ΔE, which is converted into a parameter, $\Delta E/\{t \sec(34°)\}$ where t is the detector thickness in g cm^{-2}. This is then *defined* as the linear energy transfer in silicon. The LET in tissue is then taken as 1.31 times the LET in silicon. This, of course, is not the *true* LET. The assumption that all particles have a mean angle of 34° has the following effects: (i) A normal incident true minimum ionizing particle has a LET less than the true value, (ii) fragments produced in either

detector are given an erroneous LET, as they only rarely come out in the same direction as the incident particle, and (iii) stopping particles in either detectors have an energy dependent area–solid angle product, thus leading to an erroneous flux. The effect of (i) pushes up the flux in the very low LET region, and (ii) and (iii) removes higher LET particles preferentially. This results in a lower quality factor than if these effects were not present.

The data used for model comparison comes from the flight of the DOSTEL on Shuttle flight STS-84, in $51.65° \times 389$-km orbit. The average 10.7-cm solar radio flux was 78×10^4 Jansky, and the solar modulation deceleration parameter was estimated to be 471 MV. Thus, the flight was close to the time of solar minimum. The mass shielding distribution at the telescope location is shown in Fig. 1. The telescope was positioned to have a minimum mass along the forward look direction and large shielding mass in the backward shielding direction. Thus, a majority of the trapped proton flux arrives from the forward (top) direction of the telescope. The presence of the South Atlantic

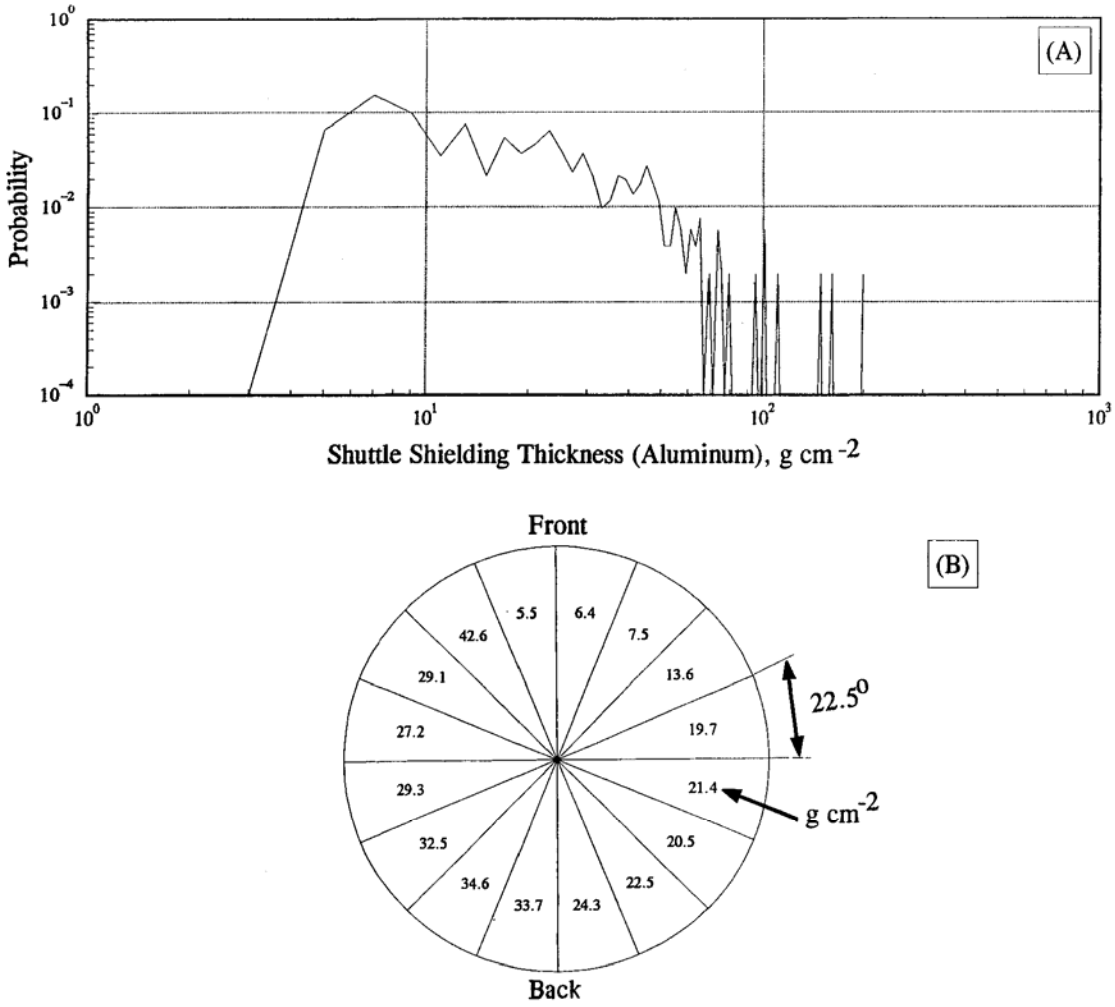

Fig. 1. (A, B) Differential Shuttle shielding distribution at the location of DOSTEL.

Anomaly (SAA) was experimentally defined as the region in space where the total count rate of all particles coming from *both* forward and backward directions was >50 particles s^{-1} or >6 particles $cm^{-2}\,sr\,s^{-1}$.

Another data set was acquired in order to study the response of single detectors, using nominal 30 and 55 MeV proton beams from Texas A&M University Cyclotron incident on a $1.8\times 1.8\,cm^2\times 500\,\mu m$ thick detector. The 55 MeV proton beam was not pure. There is a small probability of two protons hitting the detector simultaneously. These are clearly identifiable, but prevent a clear analysis of high-energy deposition events. Although the beam energy spread is less than 0.5 MeV, the true energy spectrum of beam particle hitting the detector is not fully known.

3. Modeling

Various components of the Monte Carlo modeling are described.

3.1. Radiation transport model

To understand the behavior of silicon detectors, a radiation transport model that describes the interaction of protons with silicon is required. A number of different transport models have been developed [11–16]. The works of Wilson et al. [11] and Shinn et al. [12] are based on semi-analytical approaches and use the straight-ahead approach in collision; i.e. the secondary particles continue in the direction of the incident particle. Other models are based on intranuclear cascades. The proton-induced target spallation is modeled as a two-step process, the cascade and evaporation stage. In the cascade stage, the proton, on entering the nucleus, collides with another nucleon, and this in turn collides with other nucleons. Some nucleons are ejected from the nucleus, which is left in an excited state. The excitation energy is shared by the nucleons, with the system characterized by "nuclear temperature". In the evaporation stage, the nucleons boil off isotropically in the rest frame of the nucleus. O'Neill et al. [17] combined the work of Mathews et al. [14] and Tang et al. [15] to develop the intranuclear-evaporation model. Fig. 2 shows a comparison of

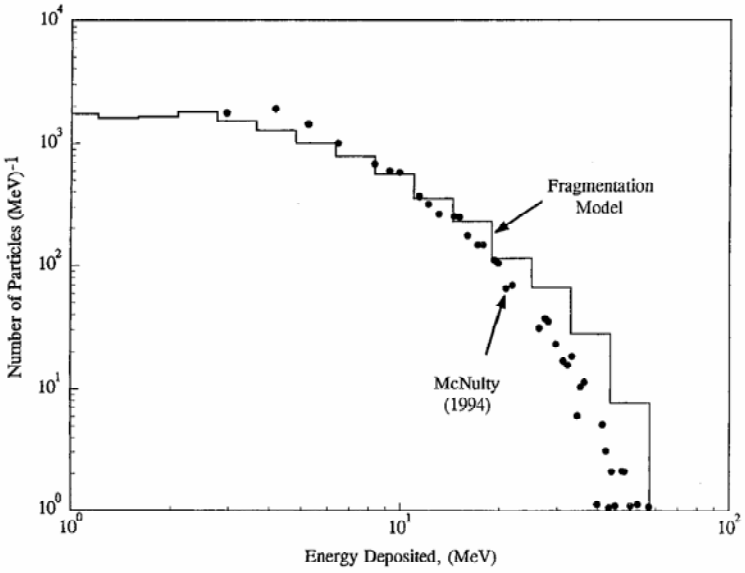

Fig. 2. A comparison of the target fragment energy deposition spectrum produced by 125 MeV protons on a 50 μm thick silicon detector and model calculated spectrum.

the calculated energy deposited in a 50 μm thick silicon detector from fragmentation products created by a 125 MeV proton beam incident normally to the detector and the experimental observations of McNulty [18]. The number of protons normally incident on the detector was known, and thus the vertical scale is absolute. The agreement between the calculated energy deposition spectrum and the measurements is good. In this paper, the O'Neill et al. [17] model is used as the radiation transport model.

3.2. Free space radiation environment

The energy spectrum of the trapped protons incident on the Space Shuttle was calculated using the AP8MIN model [19] and the IGRF 64/65 geomagnetic field model [20] and using the SPENVIS model [21]. These models go up to maximum proton energy of 300 MeV. The orbit-averaged trapped solar minimum spectrum was extended to 2 GeV by a power-law extrapolation. Fig. 3 shows a comparison of spectra calculated using these models. For proton energies greater than about 40 MeV, the two models are identical,

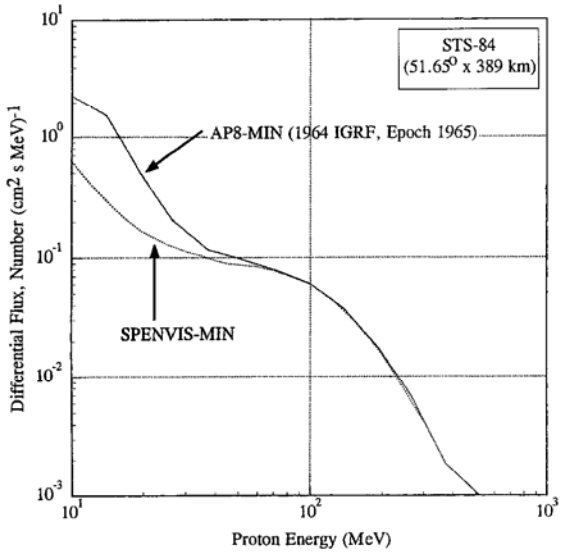

Fig. 3. A comparison of the AP8MIN/IGRF 65/65 calculated trapped spectrum with the SPENVIS calculated spectrum.

and since less than 40 MeV protons do not reach the front face of the detector due to Shuttle shielding, either model can be used for this study. The AP8MIN/IGRF 64/65 model was used. In applying the model to study the response of DOSTEL, the spectrum was transmitted through the Shuttle shielding distribution, and only those regions in space where the transmitted proton flux exceeded the threshold of 6 protons $cm^{-2} sr s^{-1}$ were considered. These regions clearly depend on the shielding distribution around the detector.

In addition to the trapped protons, there are albedo protons present. The albedo proton spectrum was measured on the June 1998 STS-91 (51.65° × 380 km) flight close to the time of the last solar minimum. This spectrum extends from 70 MeV to 12 GeV [22]. The spectrum was extended to energies lower than 70 MeV using the expression of Armstrong and Colburn [23] normalized at 70 MeV.

3.3. Energy loss distribution

The energy loss has a probability distribution that is described by the Vavilov function [24]. For thin detectors, the delta ray electrons can have sufficient energy to escape from the detector. This leads to smaller energy loss and less energy loss fluctuations. Badhwar [25] developed a modification to the Vavilov distribution to allow for electron escape. The particle path length in the detector and hence the electron energy required to escape is a function of angle. The modified theory was used to determine the actual energy loss in the detector and took this into account.

3.4. Detector geometry

The detectors are normally treated as planes. However, the actual detectors are disks of 315 μm thickness. This, therefore, allows really wide-angle particles to clip the detector edge, thus depositing far less energy than if they were to go through the full detector thickness. Protons entering from the sides of the telescope are not in the normal detector geometry; however, they can hit one of the detectors leading to a nuclear interaction that sends a reaction product to the second detector.

Such events are counted as part of the detector geometry because they satisfy the coincidence requirements. These events must be accounted for in a realistic analysis of the detector response.

4. Results

Fig. 4 shows the energy deposited by 30 and 55 MeV protons in a single detector. The solid line is the Monte Carlo distribution from a Vavilov distribution, allowing for electron escape. The absolute values of the energy deposited and widths of the distributions are well reproduced. There is slight excess of particles in the tail region of the observed distribution that is due to the spread in the incident energy spectrum.

The Monte Carlo calculations used to simulate the response of the DOSTEL were carried out as follows: first, a proton was chosen to come from either upper or lower hemisphere. Its energy was picked at random from the respective trapped proton energy spectra. The incidence angle was chosen from an isotropic angular distribution. The point of impact on the first detector was chosen at random so that it fell on the detector disk. Using

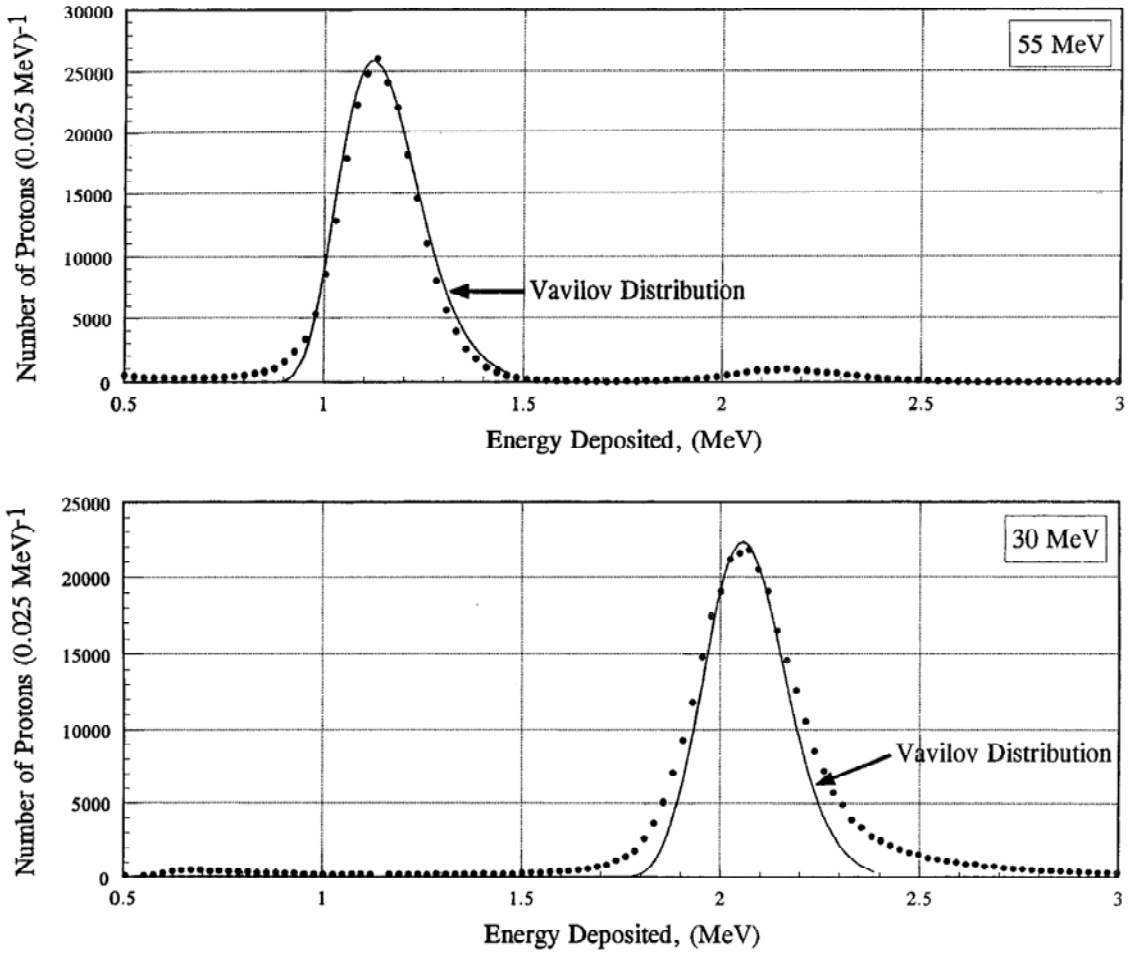

Fig. 4. A comparison of calculated and observed energy deposited spectra in 500 μm thick detector from 30 and 55 MeV normally incident protons.

an energy dependent nuclear interaction mean free path in silicon, the depth within the detector where the interaction occurred was determined. If there was no interaction in a detector, the proton was followed to the next detector and process repeated. If there was no interaction, the most probable direct ionization energy loss in the detector was determined. The actual energy deposited was chosen at random from the correct Vavilov distribution. If there was a nuclear interaction, the O'Neill et al. radiation transport model [17] was used to pick the charges and emission of angles of the fragments. Each fragment was tracked through the detector to determine the energy deposited. The total energy deposited is that due to direct ionization up to the point of interaction plus the energy deposited by the fragment. Approximately, 3 million protons per run were processed in this manner.

The albedo protons were treated in the same way, except their energy was picked from the measured albedo spectrum. Since the incident angle, θ, of each proton was known, two LET distributions were generated. In the first case the LET is defined [3] as $\Delta E/(t \sec 34°)$, where t is the detector thickness and 34° is the mean angle of particles that fall within the acceptance cone of the DOSTEL telescope, assuming an isotropic angular distribution of incident particles. In the second case $\mathrm{LET} = \Delta E/(t \sec \theta)$, where θ is the true incident angle of the particle.

Fig. 5 is a 3-D plot of the energy deposited in first detector, ED1, versus the energy deposited in the second detector, ED2. The discriminator level of 0.064 MeV cut is clear. There are less than 1% of particles in this region, mostly due to clipping trajectories. Fig. 6(A) is a projection of the same data in the ED1–ED2 plane. There is a variation of nearly four orders of magnitude in the energy deposited. The bands are the stopping particles. Fig. 6(B) is a ED1–ED2 plot in which the energy deposited is corrected for path length. The bands and main data are seen to be narrower than in Fig. 6(A), as expected.

The trapped geographic region was selected based on the counting rate of > 50 particles s^{-1}. Although this restricts the region in space to the geographic southern hemisphere, the DOSTEL

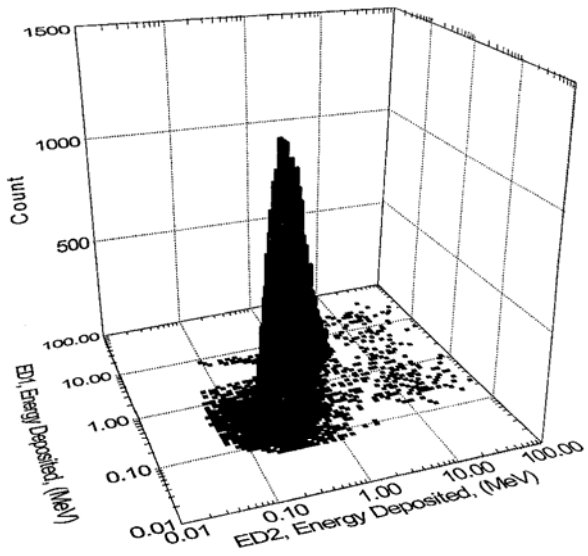

Fig. 5. A 3-D plot of the energy deposited in two of the 315 μm thick detectors by trapped + albedo protons.

still has a small contribution of GCR particles. These GCR protons, because of the geomagnetic cutoff, have energies above 400 MeV, and thus have low LET values. This contribution was added to the calculation using the GCR proton energy spectrum. Fig. 7 is a comparison of the calculated trapped LET spectrum with observations from the flight of DOSTEL on STS-84. Except for $\mathrm{LET} < 0.2\,\mathrm{keV}\,\mu\mathrm{m}^{-1}$ and LET values around 6 keV/μm (coincidence requirement), the agreement with DOSTEL measurements is quiet good. There are two other possibilities that may explain the remaining difference: (1) the high-energy portion of the AP8MIN model is in error, and (2) these are secondary pions not included in the model calculations. In either case, the increase in flux required to explain this difference appears to be excessive. The slight underestimation of flux at $\sim 6\,\mathrm{keV}\,\mu\mathrm{m}^{-1}$ is due to the treatment of the shielding around the detector itself that is not fully characterized. This is exactly the energy region where particles stop in the detector. The solid line is the calculation of Singleterry et al. [10], based on the HZETRN transport code. In the direct ionization regime, their results are in good agreement

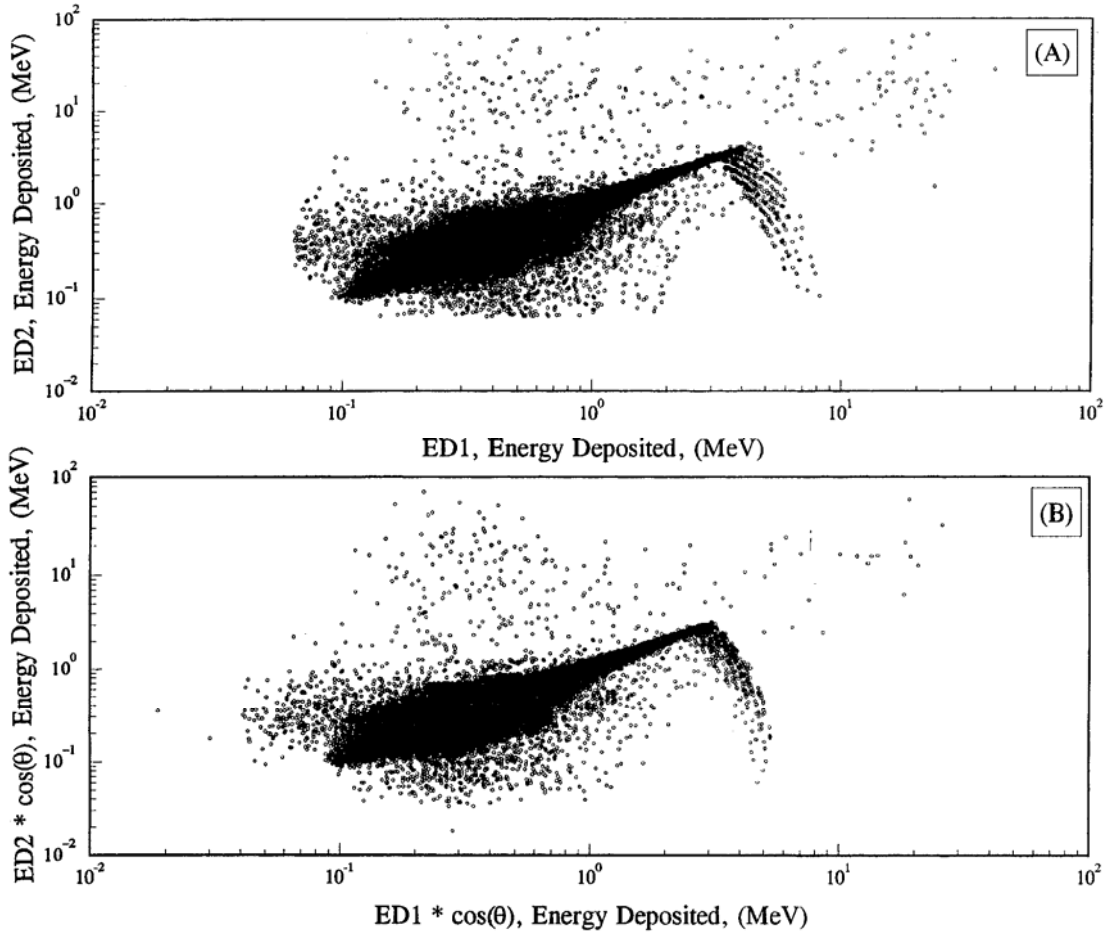

Fig. 6. (A) A cross-plot of energy deposited in the two detectors; (B) A cross-plot of path length corrected energy deposited in the two detectors.

with our calculations and with the DOSTEL observations. However, their calculations do not have particles with LET $< 0.16\,\mathrm{keV\,\mu m^{-1}}$ or $> 80\,\mathrm{keV\,\mu m^{-1}}$. In the target fragmentation regime, their calculations overestimate the flux.

Fig. 8 shows the Monte Carlo calculated LET spectra for $\langle \theta = 34 \rangle$ for trapped + albedo (Curve A), and for albedo protons (Curve B), and trapped + albedo protons for true θ (Curve C). The dose contribution of albedo protons is very small. Table 1 gives a comparison of the absorbed dose rate and radiation quality factor for each case. It shows that the assumption of an average incident angle distorts the spectrum slightly compared to the true θ spectrum, and leads to an increase of the average quality factor by 13% compared to the case using the actual θ, as will be the case in telescopes that have position-sensitive detectors, such as the RRMD and CPDS. An advantage of the Monte Carlo technique is that it allows one to examine the effect of various discriminator and coincidence setting. Putting back the particles that are "lost" due to the coincidence requirement (protons in 6.2–9.1 MeV) and ignoring the energy loss fluctuations, leads to "true" LET spectrum. This is shown as curve D. Even in this case, however, the true LET for target fragments cannot be defined, because more than

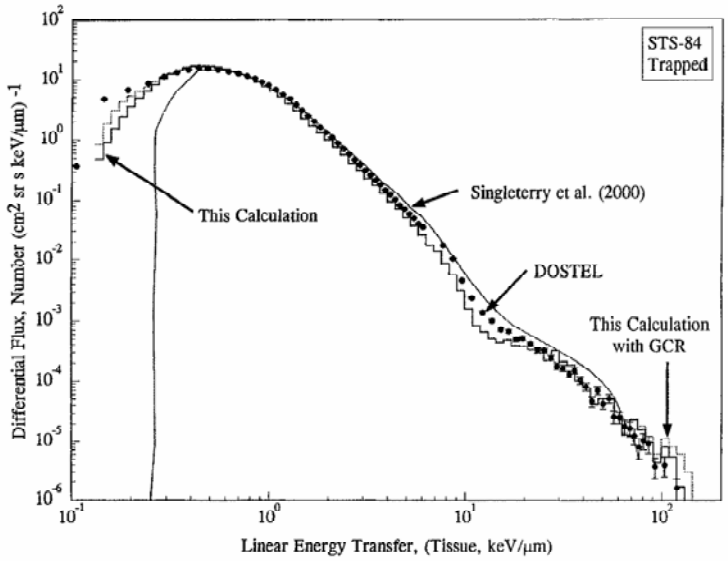

Fig. 7. A comparison of the DOSTEL measured LET spectrum with the Monte Carlo calculations and those of Singleterry et al. [10].

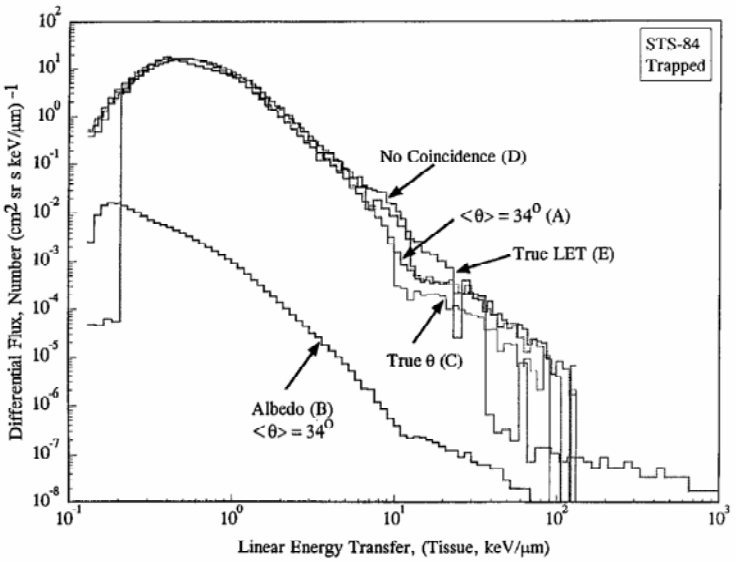

Fig. 8. Monte Carlo-based LET spectra: Histogram (A) is the total spectrum; Histogram (B) the total spectrum with true θ; Histogram (C) the albedo contribution; Histogram (D) same as (A) but no coincidence requirement; and (E) the true LET spectrum.

one fragment is typically produced and their emission angles are not known. The calculated dose rate in this idealized case is nearly the same as in other cases; however, the radiation quality factors increase significantly, being 1.45 (ICRP60) and 1.34 (ICRP26), respectively, compared to typical values of 1.1–1.2.

A TEPC was not flown on the STS-84 flight, and therefore, direct comparison with DOSTEL data is not possible. The nearest flight in time with a

Table 1
Comparison of absorbed dose and quality factor

	Dose rate (μGy/s)	Quality factor (ICRP-60)	Quality factor (ICRP-26)
DOSTEL	0.272	1.16	1.18
Singleterry et al. [10]	0.312	1.19	1.24
Monte Carlo $\langle\theta\rangle$	0.249	1.21	1.20
Monte Carlo true θ	0.244	1.07	1.09
Monte Carlo $\langle\theta\rangle$ including GCR	0.251	1.27	1.23
Monte Carlo "true" LET	0.240	1.34	1.45

TEPC on board with the same inclination as STS-84 was flight STS-81. The space weather conditions were nearly identical for these two flights. The TEPC measured linear energy spectrum extends to almost $1000\,\mathrm{keV}\,\mu\mathrm{m}^{-1}$ compared to $220\,\mathrm{keV}\,\mu\mathrm{m}^{-1}$ with an ICRP-60 quality factor of 1.73, and an ICRP-26 quality factor of 1.83, respectively. If the TEPC linear energy data range is also restricted to be $<220\,\mathrm{keV}\,\mu\mathrm{m}^{-1}$ also, then the quality factors are 1.63 and 1.67, respectively. These values are much closer to the DOSTEL values when the protons removed by the coincidence requirements are put back in. Some of the other obvious reasons for the remaining differences are: (1) The TEPC responds to secondary neutrons more efficiently than DOSTEL leading to an increase in the quality factor and there is a significant flux of secondary neutrons and protons by the trapped proton interactions with spacecraft aluminum structural material; and (2) the characteristics of target fragments in A-150 tissue equivalent plastic and silicon are obviously different; (3) since TEPC is measuring the lineal energy and DOSTEL, a surrogate of LET.

5. Conclusions

A detailed Monte Carlo technique that takes into account the detector geometry, shielding distribution, fluctuations in energy loss, angular and charge distribution of target fragmentation products, and details of the telescope design and electronics is described. It shows that: (1) There is an excellent agreement between the calculations and observations; (2) Instrumental coincidence requirements remove high LET particles, thus leading to a lower quality factor; (3) The assumption of a fixed mean angle of arrival direction of particles leads to an increase of about 13% in the quality factor compared to the case when the incident angle is known; (4) Replacing the loss of protons due to the coincidence requirements increases the quality factor significantly and brings the result in closer agreement with those from TEPC that does not require a coincidence. This Monte Carlo technique offers a powerful tool to study the response of other multi-element telescopes, determine the effect on radiation quality factor due to instrument requirements, and studies of single event upsets and latch-ups in silicon-based devices.

References

[1] Ts.P. Dachev, Yu.N. Matviichuk, J.V. Semkova, R.T. Loeva, B. Boichev, P. Baynov, N.A. Kanchev, P. Lakov, Ya.J. Ivanov, B.T. Tomov, V.M. Petrov, V.I. Redko, V.I. Kojarinov, T. Tykva, Adv. Space Res. 9 (10) (1989) 247.
[2] V.M. Petrov, I.V. Tchernyk, V.V. Benghin, A.V. Kolomensky, Yu.V. Ivanov, V.A. Shurshakov, S.A. Filippychev, V.I. Lyagushin, Proceedings of the Third Workshop on Radiation Monitoring for the International Space Station, Budapset, Hungary, 24–26 March 1998.
[3] R. Beaujean, J. Kopp, G. Reitz, Radiat. Prot. Dosim. 85 (1–4) (1999) 223.
[4] T. Doke et al., Jpn J. Appl. Phys. 35 (1996) 6241–6247.
[5] G.D. Badhwar, W. Atwell, E.V. Benton, A.L. Frank, R.P. Keegan, V.E. Dudkin, O.N. Karpov, Yu.V. Potapov, A.B. Akopva, N.V. Magradze, L.V. Melkumyan, Sh.B. Rshtuni, Radiat. Meas. 24 (1995) 283.
[6] G.D. Badhwar, F.A. Cucinotta, L.A. Braby, A. Konradi, Radiat. Res. 139 (1994) 344.
[7] G.D. Badhwar, A. Konradi, W. Atwell, M.J. Golightly, F.A. Cucinotta, J.W. Wilson, V.M. Petrov, I.V. Tchernykh, V.A. Shurshakov, A.P. Lobakov, Radiat. Meas. 26 (2) (1996) 147.
[8] ICRP, Recommendations of the International Commission on Radiological Protection, Publication 60, Annals of the ICRP, Vol. 21, No. 1–3, Pergamon Press, New York, 1991.
[9] ICRP, Recommendations of the International Commission on Radiological Protection, Publication 26, Annals of

the ICRP, Vol. 20, No. 1–3, Pergamon Press, New York, 1977.
[10] R.C. Singleterry Jr., F.F. Badavi, J.L. Shinn, F.A. Cucinotta, G.D. Badhwar, M.S. Clowdsley, J.H. Heinbockel, J.W. Wilson, W. Atwell, R. Beaujean, J. Kopp, G. Reitz, Radiat. Meas. 3(3) (2001) in press.
[11] J.W. Wilson et al., HZETRN: description of a free-space ion and nucleon transport and shielding computer program, NASA Technical Paper 3495, May 1995.
[12] J.L. Shinn et al., IEEE Trans. Nucl. Sci. NS-45 (6) (1998) 595.
[13] P.J. McNulty, W.G. Abdel-Kader, W.J. Beauvais, L. Adams, E.J. Daly, R. Harboe-Sorenson, IEEE Trans. Nucl. Sci. NS-40 (1993) 1947.
[14] G.J. Mathews, B.G. Glagola, R.A. Moyle, V.E. Viola Jr., Phys. Rev. 25 (1992) 2181.
[15] H.H.K. Tang, G.R. Srinivasan, N. Azziz, Phys. Rev. 42 (1990) 1598.
[16] K. Kwiatkowski, S.H. Zhou, T.E. Ward, V.E. Viola Jr., H. Breuer, G.J. Mathews, A. Gokmen, A.C. Mignerey, Phys. Rev. Lett. 50 (1983) 1648.
[17] P.M. O'Neill, G.D. Badhwar, W.X. Culpepper, IEEE Trans. Nucl. Sci. NS-45 (6) (1998) 2467.
[18] P.J. McNulty, W.G. Abdel-Kader, G.E. Farell, Radiat. Phys. Chem. 43 (1994) 139.
[19] D.M. Sawyer, J.E. Vette, AP8 trapped proton environment for solar maximum and solar minimum, Report NSSDC/WDC-A-R&S 76-06, NASA Goddard Space Flight Center, Greenbelt, MD, 1976.
[20] International Geomagnetic Field 1965, J. Geophys. Res. 74 (1969) 4407.
[21] D. Heynderickx, SPENVIS Space ENVironment Information System, http://www.spenvis.oma.be/, 1999.
[22] G.D. Badhwar, A.G. Troung, P.M. O'Neill, V. Choutko, Radiat. Meas. 3(3) (2001) in press.
[23] T.W. Armstrong, B.L. Colburn, Nucl. Tracks Radiat. Meas. 20 (1992) 101.
[24] P.V. Vavilov, Zh. Theor. Fiz 32 (1957) 320; JETP 5 (1957) 749.
[25] G.D. Badhwar, Nucl. Instr. and Meth. A 109 (1973) 119.